International Journal of Energy and Environmental Science
2017; 2(6): 117-126
http://www.sciencepublishinggroup.com/j/ijees
doi: 10.11648/j.ijees.20170206.11

Predicting Joint Return Period Under Ocean Extremes Based on a Maximum Entropy Compound Distribution Model

Baiyu Chen[1], Guilin Liu[2], Liping Wang[3, *]

[1]College of Engineering, University of California Berkeley, Berkeley, USA

[2]College of Engineering, Ocean University of China, Qingdao, China

[3]School of Mathematical Sciences, Ocean University of China, Qingdao, China

Email address:

wlpjsh@163.com (Liping Wang)

[*]Corresponding author

To cite this article:

Baiyu Chen, Guilin Liu, Liping Wang. Predicting Joint Return Period Under Ocean Extremes Based on a Maximum Entropy Compound Distribution Model. *International Journal of Energy and Environmental Science*. Vol. 2, No. 6, 2017, pp. 117-126.
doi: 10.11648/j.ijees.20170206.11

Received: October 7, 2017; **Accepted**: November 8, 2017; **Published**: December 11, 2017

Abstract: In this paper, we proposed a novel 2-dimensional (2D) distribution model based on the maximum-entropy (ME) principle to predict the joint return period under ocean extremes. In detail, we first derive the joint probability distribution of the extreme wave heights and the extreme water-levels during a typhoon by using the maximum-entropy principle, and then we nest this distribution with the maximum-entropy distribution of discrete variables to form such a maximum-entropy 2-dimensional (ME 2D) compound distribution model. To evaluate the performance of our model, we conduct experiments to predict the N-year joint return-periods of the extreme wave heights and the extreme water levels in two areas of the East China Sea. According to the experimental results, our model performs better in predicting in the highly unpredictable joint probability of extreme wave heights and water levels in typhoon affected sea areas, compared with the widely-used Poisson-Mixed-Gumbel model in ocean engineering design. This ascribes to the fact that unlike other models whose corresponding parameters are arbitrarily assigned, our model utilizes both the new 2D distribution and the discrete distribution which are based on the ME principle.

Keywords: Maximum Entropy Principle, 2D Compound Distribution Model, Extreme Wave Height, Extreme Water Level, Optimization, Climate Change

1. Introduction

Global warming causes both the occurrence-frequency and intensity of typhoon tend to increase [1]. Specifically, in coastal zones, typhoons cause disasters mainly in two forms [2]: (a) large waves that turn over ships and destroy marine structures and breakwaters, and (b) heavy rain and storm surge that cause anomalously high water-levels. These two forms are especially frequently observed in estuary and shallow bay areas, and hence low lands would be submerged. When extreme waves superpose on extreme waters levels, an extreme disaster would occur, which is one of the main mechanisms through which Hurricane Katrina (2005) caused serious disaster in New Orleans. Therefore, it is important for ocean-engineering designs and disaster preventions to rationally predict the joint return-period of extreme wave heights and extreme water levels.

Motivated by these requirements, in this paper, the maximum-entropy principle is used to derive the joint probability distribution of the extreme wave heights and the extreme water-levels during a typhoon. Then, we nest this distribution with the maximum-entropy distribution of discrete variables, derived by Wang et al. [3] to describe the probability of annual typhoon frequency, to form a new compound distribution model. Theoretically, the compound distribution is better than the Poisson-Logistic model and the Poisson-Mixed-Gumbel model [4, 5, 12] when describing the highly-unpredictable joint probability of extreme wave heights and extreme water-levels in typhoon-affected sea

areas. This is because that our model is based on maximum-entropy principle and it takes the effect of typhoon frequency into account. Furthermore, the proposed compound distribution used in our model also helps to address a major drawback of widely used Poisson-Logistic model and Poisson-Mixed-Gumbel model, i.e., extremely higher apriority during prediction which is caused by arbitrarily assigning the two-dimensional distribution [6-11].

To evaluate the advantages of our compound model, we use both the proposed compound model and the Poisson-Mixed-Gumbel model to predict the N-year joint return-period of extreme wave heights and extreme water-levels in the Maidao and Chaoliandao sea areas of the East China Sea, and then compare their corresponding results.

The rest of this paper is organized as follows: the derivation of the maximum-entropy two-dimensional joint distribution is presented in Section 2. Details of the new compound model is presented in Section 3. Evaluation of our model is presented in Section 4. Lastly, conclusions are summarized in Section 5.

2. The Maximum-Entropy Two-Dimensional Joint Distribution

2.1. Derivation

Assume the wave in a typhoon affected sea area can be described by a two-dimensional (abbreviated as 2D hereinafter) random vector *(X, Y)*, where extreme wave height is *X*, and the extreme water level is *Y*, and *X* and *Y* are neither independent nor synchronous, but correlated to a certain extent.

The 2D joint information entropy (abbreviated as entropy hereinafter) can defined as:

$$H(f) = -\int_R \int_R f(x,y)\log f(x,y)dxdy \tag{1}$$

where *f(x, y)* is the joint probability density function of *X* and *Y*. Let *P* denote a kind of probability density functions. If there exist such a $p_0 \in P$ that for any $f \in P$

$$H(p_0) = \max\{H(f) : f \in P\} \tag{2}$$

then $H(p_0)$ is the maximum entropy of *P*, and p_0 is called the maximum entropy probability density function (the term 'maximum entropy' is abbreviated to 'ME' hereinafter). The ME principle [12-15] is applied to deriving ME 1D distributions to describe the probability of extreme wave heights, extreme water levels or others [16-25] and obtained relatively better results.

According to the definition given above, the ME 2D probability density function *f(x, y)* is such a function as to maximize *H(f)* shown in Eq. (1). Obviously, how to solve such a *f(x, y)* from Eq. (1) is a 2D variation problem. Since solving a variation problem needs constraint conditions, for this problem, we can propose the following constraints:

$$\int_0^{+\infty}\int_0^{+\infty} f(x,y)\mathrm{d}x\mathrm{d}y = 1 \tag{3}$$

$$\int_0^{+\infty}\int_0^{+\infty} f(x,y)(\ln x + \ln y)\mathrm{d}x\mathrm{d}y = c_1 < +\infty \tag{4}$$

$$\int_0^{+\infty}\int_0^{+\infty} x^{m_1} f(x,y)\mathrm{d}x\mathrm{d}y = c_2 < +\infty \tag{5}$$

$$\int_0^{+\infty}\int_0^{+\infty} y^{m_2} f(x,y)\mathrm{d}x\mathrm{d}y = c_3 < +\infty \tag{6}$$

where m_1 and m_2 are two positive integers or positive fractions, and c_1, c_2 and c_3 are three constants. In the above equations, the lower limits of integrals are taken to be zero, because both the extreme wave height and extreme water level are nonnegative. Notice that the above four constraints are in accordance with axioms and generally acknowledged truth rather than *a priori*. Constraint (3) is imperative for the regularity of probability density functions. Constraint (4) ensures that $f(x,y) \to 0$ in the following conditions: $x \to \infty$ and $y \to \infty$; $x \to 0$ and $y \to 0$; $x \to 0$ and *y=constant*; and $y \to 0$ and x=constant, which are in accordance with generally acknowledged fact. The constraints (5) and (6) ensure, on one hand, that $f(x,y) \to 0$ when $x \to +\infty$ or $y \to +\infty$. On the other hand, that any order moments of *f(x, y)* and any order moments of its marginal distributions exist (see Appendix for the proof).

The ME 2D joint probability density function *f(x, y)* derived in this paper is to maximize *H(f)* shown in Eq. (1) under the constraints (3), (4), (5) and (6). However, finding such a *f(x, y)* is a generalized isoperimetric variation problem. According to the theorem of variation, such a *f(x, y)* should satisfy the Euler equation:

$$\frac{\partial L}{\partial f(x,y)} = 0 \tag{7}$$

where

$$L = -f(x,y)\ln f(x,y) + tf(x,y) + bf(x,y)(\ln x + \ln y) - cx^{m_1} f(x,y) - dy^{m_2} f(x,y)$$

that is determined by the variation problem regarding the functional:

$$\begin{aligned} J = &\int_0^{+\infty}\int_0^{+\infty} -f(x,y)\ln f(x,y)\mathrm{d}x\mathrm{d}y + t\left(\int_0^{+\infty}\int_0^{+\infty} f(x,y)\mathrm{d}x\mathrm{d}y - 1\right) \\ &+ b\left[\int_0^{+\infty}\int_0^{+\infty} f(x,y)(\ln x + \ln y)\mathrm{d}x\mathrm{d}y - c_1\right] \\ &- c\left[\int_0^{+\infty}\int_0^{+\infty} x^{m_1} f(x,y)\mathrm{d}x\mathrm{d}y - c_2\right] \\ &- d\left[\int_0^{+\infty}\int_0^{+\infty} y^{m_2} f(x,y)\mathrm{d}x\mathrm{d}y - c_3\right] \end{aligned} \tag{8}$$

where *t, b, c* and *d* are parameters.

From Eq. (7) we also obtain:

$$-\ln f(x,y)-1+t+b\ln xy-cx^{m_1}-dy^{m_2}=0$$

which follows:

$$f(x,y)=e^{t-1}e^{b\ln xy}e^{-cx^{m_1}-dy^{m_2}}$$

With $\alpha=e^{t-1}$, thus we have

$$f(x,y)=a(xy)^b e^{-cx^{m_1}-dy^{m_2}} \tag{9}$$

To sum up, Eq. (9) is the ME 2D joint distribution derived in the paper which has many parameters. These parameters enable our model to fit the observed data more flexibly and precisely in comparison with other traditional distribution models.

2.2. Determination of the Parameters

In this subsection, we focus on to determine the six parameters from Eq. (9), i.e., m_1, m_2, α, b, c and d. According to the ME principle stated above, these parameters should make the distribution most suitable to fitting observed data. Thus, we claim that these parameters should be determined in the following manner:

At first, a set of equations are derived from Eq. (9) to relate these parameters with the joint moments $\mathrm{E}(x^m, y^n)$ defined as:

$$\mathrm{E}(x^m,y^n)=\int_0^{+\infty}\int_0^{+\infty}x^m y^n \alpha(xy)^b e^{-cx^{m_1}-dy^{m_2}}\mathrm{d}x\mathrm{d}y$$

$$=\alpha\int_0^{+\infty}\int_0^{+\infty}x^{m+b}y^{n+b}e^{-cx^{m_1}-dy^{m_2}}\mathrm{d}x\mathrm{d}y \tag{10}$$

where m and n are integers, and then these moments are estimated from available data, and finally these parameters are numerically solved from these equations.

Let $u=cx^{m_1}, v=dy^{m_2}$. Eq. (10) can be rewritten as

$$\mathrm{E}(x^m,y^n)=\alpha\int_0^{+\infty}\frac{1}{m_1}c^{-\frac{m+b+1}{m_1}}u^{\frac{m+b+1}{m_1}-1}e^{-u}\mathrm{d}u\cdot\int_0^{+\infty}\frac{1}{m_2}d^{-\frac{n+b+1}{m_2}}u^{\frac{n+b+1}{m_2}-1}e^{-v}\mathrm{d}v \tag{11}$$

and completing the integrations we have

$$\mathrm{E}\left(x^m,y^n\right)=\frac{\alpha}{m_1m_2c^{\frac{m+b+1}{m_1}}d^{\frac{n+b+1}{m_2}}}\Gamma(\frac{m+b+1}{m_1})\Gamma(\frac{n+b+1}{m_2}) \tag{12}$$

where $\Gamma(.)$ is the Gamma function defined as

$$\Gamma(\lambda)=\int_0^{+\infty}e^{-x}x^{\lambda-1}dx\,.$$

With $T_{m,n}$ denoting $\mathrm{E}(x^m,y^n)$, we have from Eq. (12) that

$$\begin{cases}\dfrac{T_{1,0}^{\ 2}}{T_{0,0}T_{2,0}}=\dfrac{\Gamma^2(\frac{b+2}{m_1})}{\Gamma(\frac{b+1}{m_1})\Gamma(\frac{b+3}{m_1})}\\ \dfrac{T_{0,1}^{\ 2}}{T_{0,0}T_{0,2}}=\dfrac{\Gamma^2(\frac{b+2}{m_2})}{\Gamma(\frac{b+1}{m_2})\Gamma(\frac{b+3}{m_2})}\\ \dfrac{T_{1,1}^{\ 2}}{T_{2,0}T_{0,2}}=\dfrac{\Gamma^2(\frac{b+2}{m_1})\Gamma(\frac{b+2}{m_2})}{\Gamma(\frac{b+1}{m_1})\Gamma(\frac{b+3}{m_1})\Gamma(\frac{b+1}{m_2})\Gamma(\frac{b+3}{m_2})}\end{cases} \tag{13}$$

and that

$$\frac{T_{1,0}}{T_{0,0}}=c^{-\frac{1}{m_1}}\frac{\Gamma(\frac{b+2}{m_1})}{\Gamma(\frac{b+1}{m_1})} \tag{14}$$

$$\frac{T_{0,1}}{T_{0,0}}=d^{-\frac{1}{m_2}}\frac{\Gamma(\frac{b+2}{m_2})}{\Gamma(\frac{b+1}{m_2})} \tag{15}$$

Hence, we have:

$$c=\left[\frac{\Gamma(\frac{b+2}{m_1})T_{0,0}}{\Gamma(\frac{b+1}{m_1})T_{1,0}}\right]^{m_1} \tag{16}$$

$$d=\left[\frac{\Gamma(\frac{b+2}{m_2})T_{0,0}}{\Gamma(\frac{b+1}{m_2})T_{0,1}}\right]^{m_2} \tag{17}$$

On the other hand, since

$$T_{0,0}=\int_0^{+\infty}\int_0^{+\infty}f\left(x,y\right)dxdy=1$$

substituting 1 for $T_{0,0}$ in the equation

$$\mathrm{E}\left(x^0, y^0\right) = T_{0,0} = \frac{\alpha}{m_1 m_2 c^{\frac{b+1}{m_1}} d^{\frac{b+1}{m_2}}} \Gamma(\frac{b+1}{m_1})\Gamma(\frac{b+1}{m_2})$$

we obtain

$$\alpha = \frac{m_1 m_2 c^{\frac{b+1}{m_1}} d^{\frac{b+1}{m_2}}}{\Gamma(\frac{b+1}{m_1})\Gamma(\frac{b+1}{m_2})} \tag{18}$$

Thus, from Eqs. (13), (16), (17) and (18) we can numerically solve the parameters m_1, m_2, b, c, d and α in the ME distribution shown in Eq. (9), as long as the moments $T_{i,j}$ are determined. As usually done in practical statistics, the mixed moments $T_{i,j}$ are estimated from observed data (x_i, y_j), $i, j=1, 2, \ldots, N$ by using the formula:

$$T_{m,n} \approx \frac{\sum_{i,j=1}^{N} x_i^{\,m} y_j^{\,n}}{N^2} \tag{19}$$

The procedure of solving these parameters is as follows: First substitute $T_{i,j}$ in Eq. (13) with the mixed moments estimated by Eq. (19), so that the parameters m_1, m_2 and b can be numerically solved; Next, substitute m_1, b and m_2, b into Eq. (16) and Eq. (17), respectively. Finally, we can obtain c and d and α from Eq. (18).

3. The ME 2D Compound Distribution Model

The concept of compound distribution has been widely applied to predicting the N-year return-period wave-height, water-level or others in typhoon-affected sea areas [1-3]. Recently, it was extended to multi-dimensional compound distribution to describe joint probabilities of several ocean random variables [13]. The explicit expression of 2D compound distribution is as [18-21]:

$$F(x,y) = P_0 + \sum_{i=1}^{\infty} P_i \cdot i \cdot \int_{-\infty}^{y}\int_{-\infty}^{x} G_x^{\,i-1}(u) g(u,v)\, dudv \tag{20}$$

where P_i is the probability of a discrete random variable, $g(u, v)$ is the joint probability density function of the 2D random vector $(X. Y)$, $G_x(u)$ is the marginal distribution function of $(X. Y)$ that is, $G_x(u) = G(u, +\infty)$ (where $G(u, v)$ is the distribution function corresponding to $g(u, v)$).

The so-called ME distribution for a discrete random variable i taking only positive integral values,

$$p_i = \eta i^{\gamma} \exp\{-\beta i^{\xi}\},\ i = 0,1,2,\cdots \tag{21}$$

was derived on the ME principle by [2, 3, 10] with the constraints

$$\begin{cases} \sum_{i=0}^{\infty} p_i = 1\ ,\ p_i \geq 0 \\ \sum_{i=0}^{\infty} i^{\xi} \cdot p_i < +\infty \\ \sum_{i=0}^{\infty} \ln i \cdot p_i < +\infty \end{cases} \tag{22}$$

where η, β, γ and ξ are parameters to be determined. The equations derived for determining these parameters are as follows:

$$\begin{cases} \dfrac{A_1^2}{A_0 A_2} = \dfrac{\Gamma(\frac{\gamma+2}{\xi})^2}{\Gamma(\frac{\gamma+1}{\xi})\Gamma(\frac{\gamma+3}{\xi})} \\ \dfrac{A_0 A_3}{A_1 A_2} = \dfrac{\Gamma(\frac{\gamma+4}{\xi})\Gamma(\frac{\gamma+1}{\xi})}{\Gamma(\frac{\gamma+2}{\xi})\Gamma(\frac{\gamma+3}{\xi})} \\ \beta = [\dfrac{A_1 \Gamma(\frac{\gamma+1}{\xi})}{\Gamma(\frac{\gamma+2}{\xi})}]^{-\xi} \\ \ell = \ln[\dfrac{\beta^{\frac{\gamma+1}{\xi}} \cdot \xi}{\Gamma(\frac{\gamma+1}{\xi})}] + 1 \end{cases} \tag{23}$$

where A_k (k=1, 2 and 3) is the k th-order moment, as,

$$A_k = \mathrm{E}\left(i^k\right) = \sum_{i=0}^{\infty} i^k p_i,\ k = 0,1,2,\cdots \tag{24}$$

In practical, A_k is estimated based on the observed data by using the following equation:

$$\overline{A_k} = \frac{1}{N}\sum_{i=0}^{N} i^k,\ k = 0,1,2,\cdots N \tag{25}$$

With A_k in Eq. (24) substituted by $\overline{A_k}$, the parameters η, β, γ and ξ can be numerically solved from Eq. (23).

The ME 2D compound distribution model proposed in this paper is formed in accordance with Eq. (20) by taking $f(x, y)$ shown in Eq. (9) to be $g(u, v)$ to describe the joint probability of extreme wave heights and extreme water levels, and p_i (Eq. (1)) is simply the probability of having i typhoons in a single year (i is referred to as annual occurrence frequency), and the resulting model is:

$$F(x,y) = P_0 + \sum_{i=1}^{\infty} \eta \cdot i^{\gamma+1} \cdot \exp\{-\beta i^{\xi}\} \int_{-\infty}^{y}\int_{-\infty}^{x} G_x^{\,i-1}(u) g(u,v)\, dudv \tag{26}$$

where

$$g(u,v)=\alpha(uv)^b e^{-cu^{m_1}-dv^{m_2}}$$

$$G_x(u)=\int_0^u\int_0^{+\infty}\alpha(xy)^b e^{-cx^{m_1}-dy^{m_2}}dydx$$

and α, m_1, m_2, b, c, d, η, β, γ and ξ are parameters to be determined.

4. Evaluation

In this section, we evaluate the proposed model (as shown in Eq. (26)) to predict the joint return-period of extreme wave heights and water levels in Maidao and Chaoliandao sea areas near Qingdao.

The data of annual extreme wave height and extreme water level are obtained from Maidao hydrometric station (36°03′N, 120°25′E) (1984-2001) and Chaoliandao hydrometric station (35°53′N, 120°52′E) (1965-1989). These data are used to determine the parameters α, m1, m2, b, c and din Eq. (26), that is, the parameters in the ME 2D joint distribution shown in Eq. (9). According to the procedure presented in Section2, these parameters are computed and listed in Table 1.

Table 1. *Derived parameters of the joint distribution of the extreme wave heights and extreme water levels during typhoons in two different locations.*

Para.	α	b	c	d	m_1	m_2
Maidao	.14×105	2.80×10	6.22×10	9.38×10^{-7}	3.06×10^{-1}	2.28×10
Chaoliandao	1.83×10^{-5}	3.52	3.22×10^{-7}	1.25×10^{-4}	11	5.11

The annual typhoon occurrence-frequencies of Maidao sea area (1984-2001) and Chaoliandao sea area (1965-1989) are listed in Table 2. From these data, the parameters η, β, γ and ξ in Eq. (26) numerically computed from Eq. (23) and Eq. (25) are listed in Table 3.

Table 2. *The observed annual typhoon occurrence-frequencies of Maidao and Chaoliandao.*

	Maidao (1984-2001)								Chaoliandao (1965-1989)							
Annual occurrence-frequency	**1**	**2**	**3**	**4**	**5**	**6**	**7**	**8**	**1**	**2**	**3**	**4**	**5**	**6**	**7**	**8**
Occurrence number of year	2	3	3	5	5	0	1	1	4	6	6	7	2	1	0	1
Total number of years	20								27							
Total occurrence-times	77								86							

Table 3. *The computed parameters of the joint distribution of the extreme wave heights and extreme water levels during typhoons in two different locations.*

Maidao				Chaoliandao			
η	**β**	**γ**	**ξ**	**η**	**β**	**γ**	**ξ**
7.92×10^{-2}	1.94×10^{-2}	1.17	2.54	2.09×10^{-1}	4.87×10^{-1}	2.03	1.30

Figure 1 and Figure 2 show the ME joint distributions of extreme wave heights and extreme water levels in Maidao and Chaoliandao sea areas, respectively.

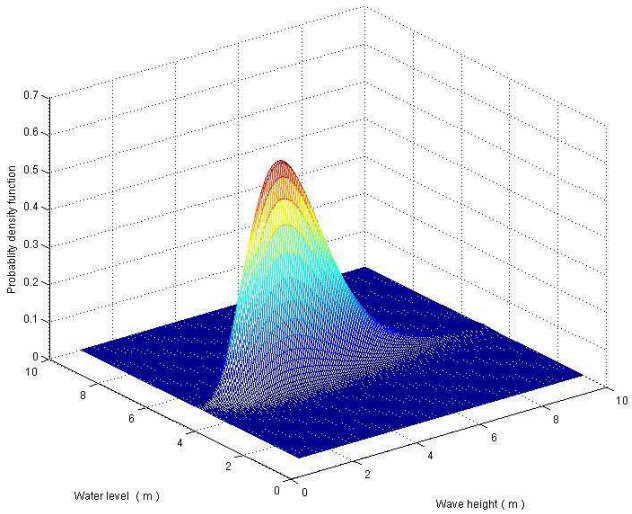

Figure 1. *ME joint distributions of extreme wave heights and extreme water levels in Maidao area.*

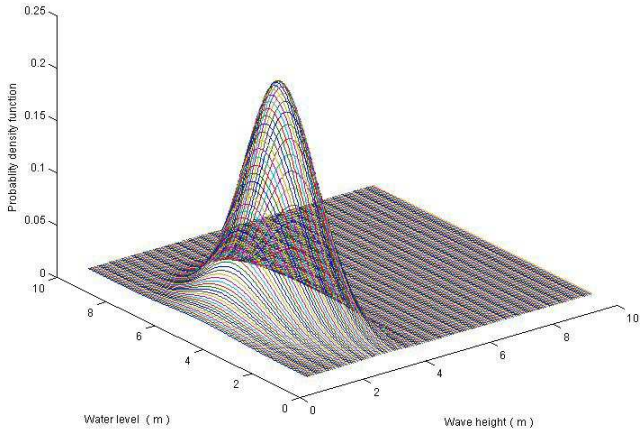

Figure 2. *ME joint distributions of extreme wave heights and extreme water levels in Chaoliandao area.*

As shown in Eq. (26), the marginal distribution, i.e.,

$$G_x(u)=\int_0^u\int_0^{+\infty}\alpha(xy)^b e^{-cx^{m_1}-dy^{m_2}}dydx$$

is the ME distribution function of extreme wave heights, and the other marginal distribution, i.e.,

$$G_y(v) = \int_0^v \int_0^{+\infty} \alpha(xy)^b e^{-cx^{m_1} - dy^{m_2}} dxdy$$

is the ME distribution function of extreme water level. Figures 3 and 4 illustrate the comparison of the two distribution functions with observed data for Maidao sea area, and Figures 5 and 6 show the same comparison for Chaoliandao sea area. As can be seen from these figures, the proposed distribution curves can accurately fit the data.

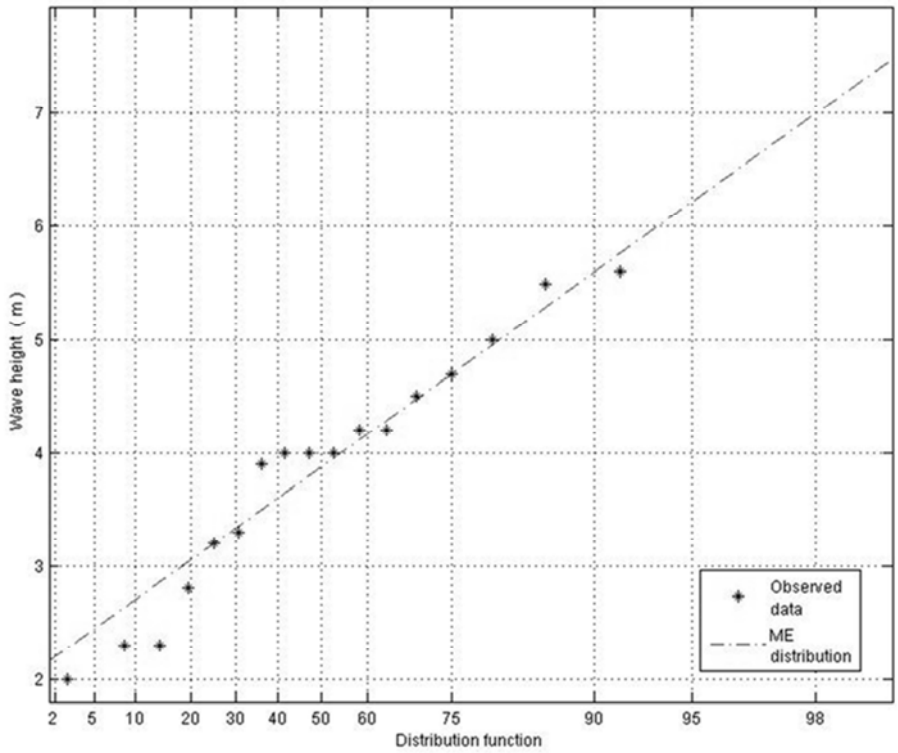

Figure 3. *ME distribution of extreme heights (Maidao sea area).*

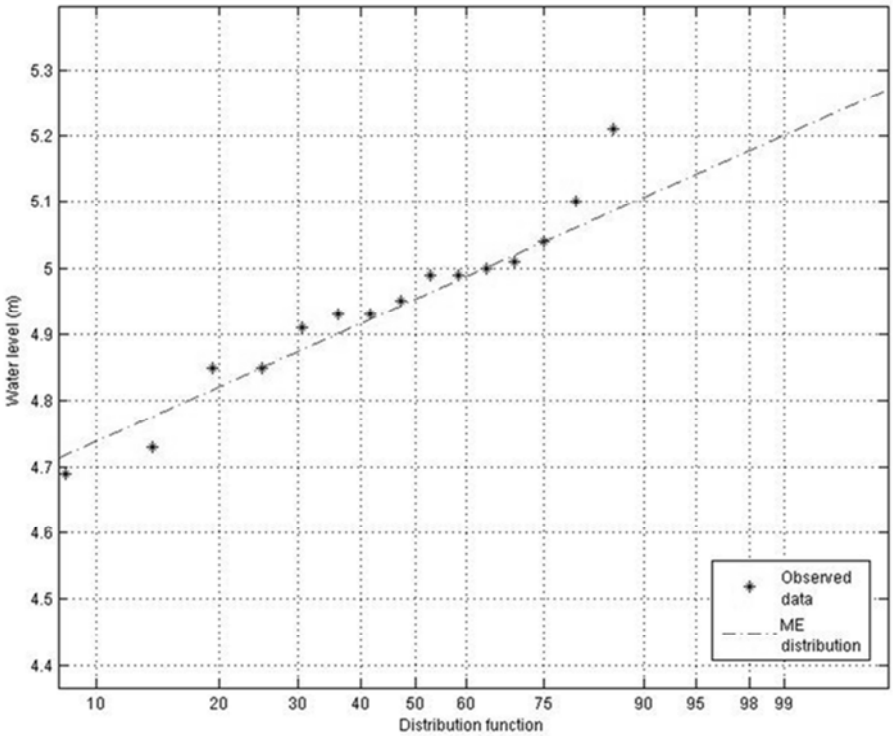

Figure 4. *ME distribution of extreme water levels (Maidao sea area).*

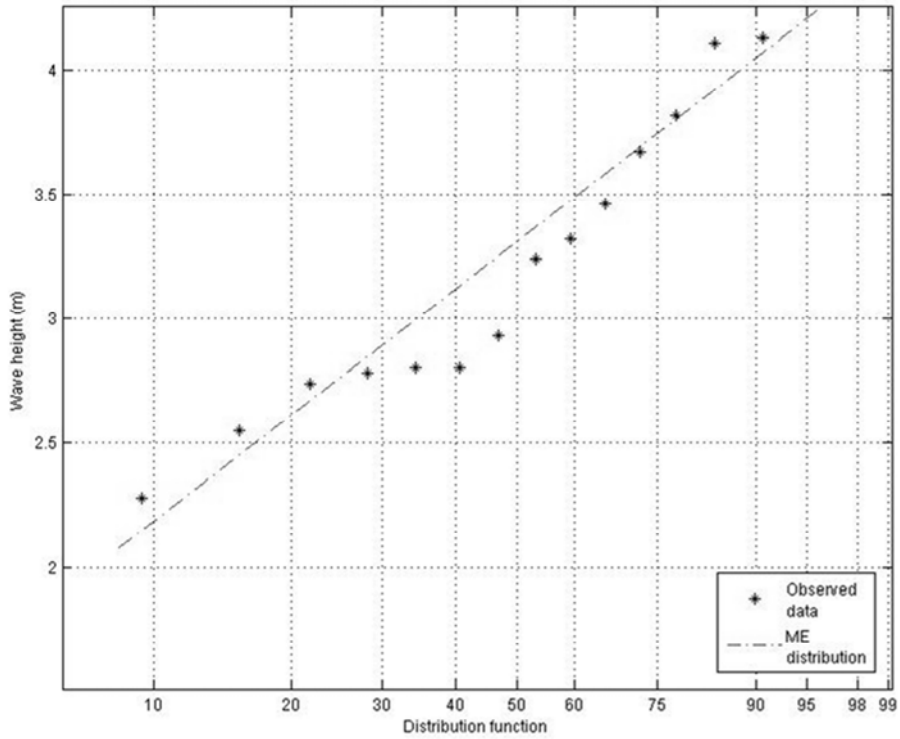

Figure 5. *ME distribution of extreme heights (Chaoliandao sea area).*

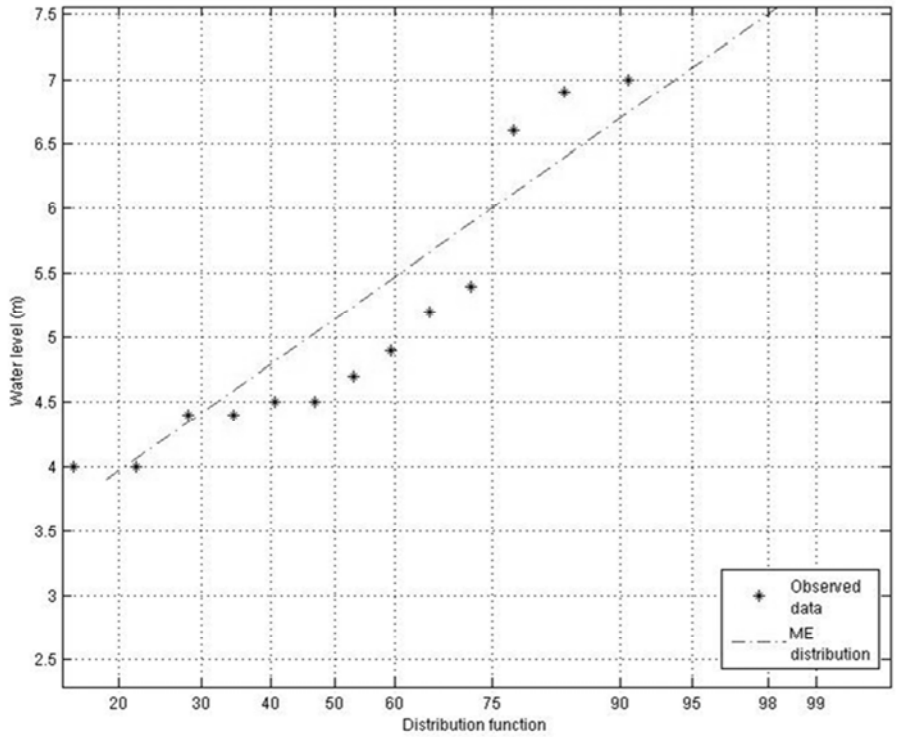

Figure 6. *ME distribution of extreme water levels (Chaoliandao sea area).*

Figures 7, 8 and Figures 9, 10 show the comparisons of the ME 2D distribution shown in Eq. (9) with the Logistic 2D distribution and Gumbel 2D distribution, respectively. The last two distributions have been widely used as the models to describe the joint probability of two extremes in marine studies. It is seen from the Figures 7 and 8 that overall, the ME 2D distribution fits the data obviously better than the Logistic distribution, especially for the middle values where the data are concentrated.

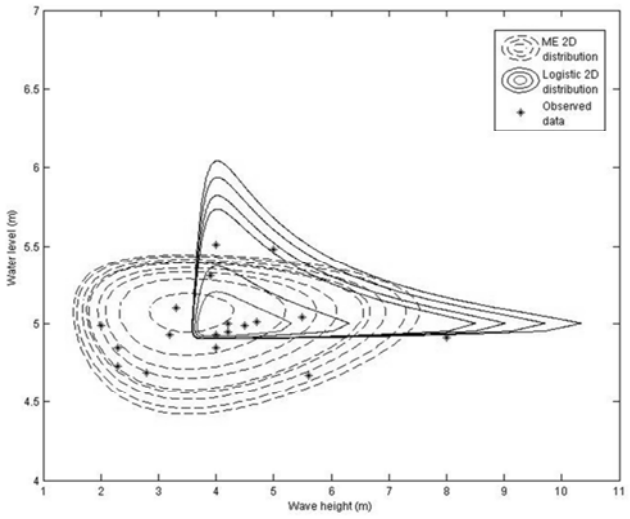

Figure 7. *Comparison of the ME 2D distribution with the Logistic 2D distribution (Maidao sea area).*

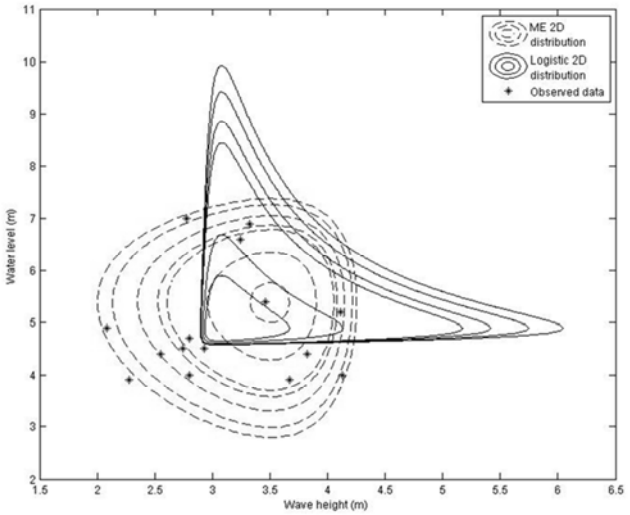

Figure 8. *Comparison of the ME 2D distribution with the Logistic 2D distribution (Chaoliandao sea area).*

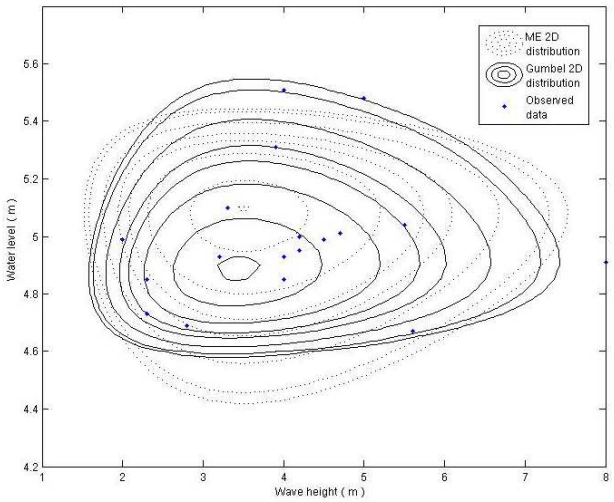

Figure 9. *Comparison of the ME 2D distribution with the Gumbel 2D distribution (Maidao sea area).*

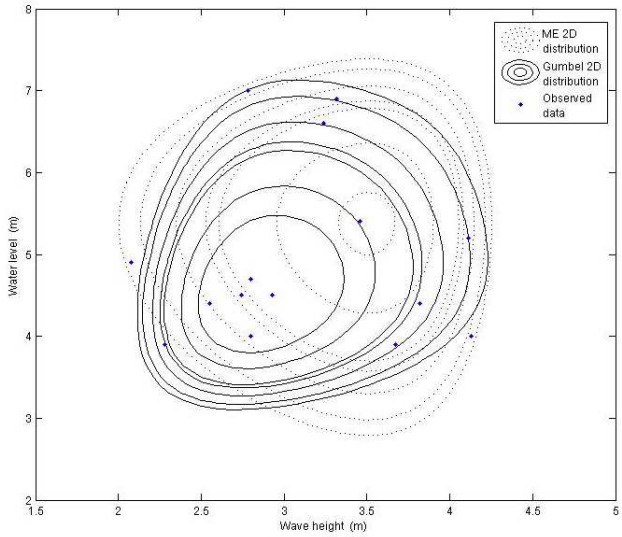

Figure 10. *Comparison of the ME 2D distribution with the Logistic 2D distribution (Chaoliandao sea area).*

In addition, Figures 9, 10 further show that the fitting results of ME 2D distribution and Gumbel 2D distribution are similar, but the former is a little better than the latter.

With the joint 2D distribution function denoted by $F(x, y)$ and its marginal distributions denoted by $F_x(x)$ and $F_y(y)$, respectively, the joint return period N (years) of the extreme wave height X and extreme water level Y is defined as,

$$N = \frac{1}{P(X > x, Y > y)} = \frac{1}{1 - F_x(x) - F_y(y) + F(x, y)} \quad (27)$$

From the ME compound distribution model $F(x, y)$ shown in Eq. (26), the isograms of N are computed for the Maidao and Chaoliandao sea areas and shown in Figure 11 and Figure 12, respectively.

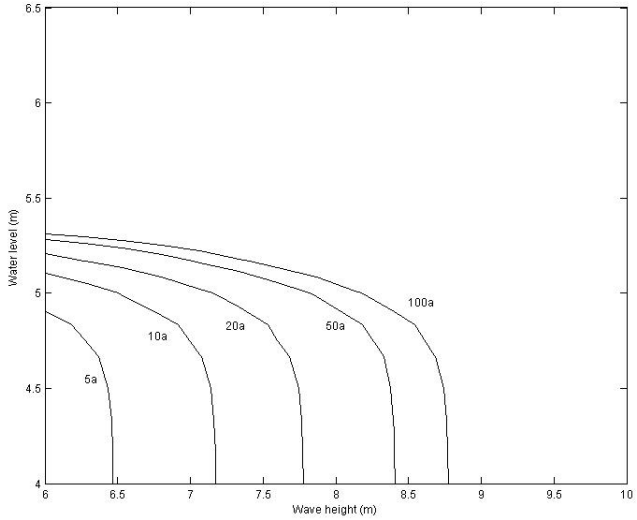

Figure 11. *Isograms of joint return period of the extreme wave height and extreme water level (maidao sea area).*

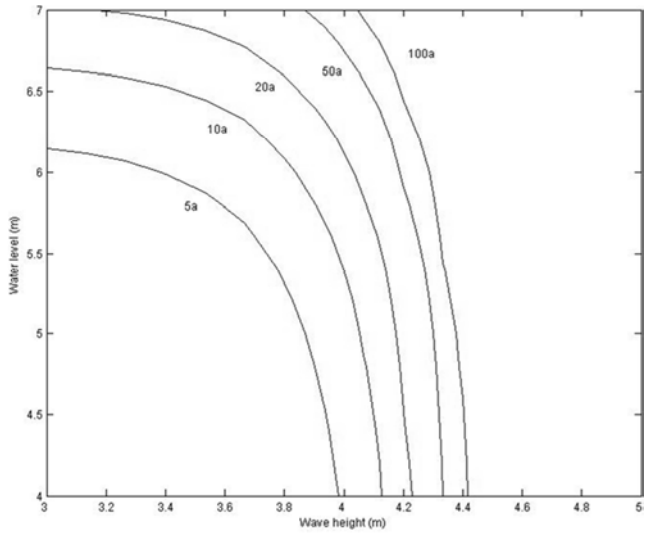

Figure 12. *Isograms of joint return period of the extreme wave height and extreme water level (Chaoliandao sea area).*

As the model shown in Eq. (26) is of two-dimensional distribution, different combinations of extreme wave height and extreme water level can result in identical *N*. As usually conducted in ocean engineering, the design wave height and water level are predicted in the following manner: the wave height is regarded as a prior variable in the model and the ME 2D compound distribution corresponding to the model is used to predict the *N*-year return-period wave heights, and then to solve its corresponding water levels from the model (26) and Eq. (27). Additionally, the prediction results of Maidao and Chaoliandao sea areas by using the Poisson-Mixed-Gumbel model and our proposed model are listed in Table 4.

In detail, the wave-height values listed in Table 4 are predicted by regarding the wave height as a prior variable and using the ME 1D compound distribution model, respectively, as a result, these values are of the *N*-year return-period extreme wave height. The water level values listed in Table 4 are predicted by using the ME two-dimensional compound distribution model shown in Eq. (26) and assuming these wave-height values. For example, the first wave-height value 7.38m in the table is the 10-year return-period extreme wave height in Maidao sea area, while its corresponding water-level value 5.51m is the 10-year return-period extreme water level.

Table 4. *N-year joint return-period wave heights and water levels calculated using Poisson-Mixed-Gumbel Model and Present Model at two different locations.*

		Poisson-Mixed-Gumbel model				Present model			
Joint return period (*N* years)		**10a**	**20a**	**50a**	**100a**	**10a**	**20a**	**50a**	**100a**
Maidao	Wave height (m)	7.38	8.07	8.98	9.73	7.38	8.07	8.98	9.73
	Water level (m)	5.51	5.57	5.63	5.67	5.41	5.46	5.49	5.52
Chaoliandao	Wave height (m)	4.42	4.63	4.88	5.04	4.42	4.63	4.88	5.04
	Water level (m)	7.78	8.34	9.04	9.54	6.80	7.09	7.49	7.74

As can be seen from Table 4, the water-level values of Maidao sea area predicted by the present model are close to those predicted by the Poisson-Mixed-Gumbel model, while for Chaoliandao sea area, the water-level values predicted by Poisson-Mixed-Gumbel model are so high that the 20-year joint return-period water level reaches 8.34m. As Chaoliandao is an islet and located in open sea, the extreme water levels occurring in its surrounding sea area should be lower than those occurring in river mouth and bayou sea areas. In fact, the highest water level observed in the past 25 years (from 1965 to 1989) is merely 6.90m. Obviously, such high water level are over estimated. Additionally, for both Maidao and Chaoliandao sea areas, the water-level values predicted by the present model are relatively reasonable, which validates the advantage of the present model.

5. Conclusions

In this paper, we developed a 2D distribution model for the joint return period under ocean extremes prediction problem. Our model is based on the maximum-entropy (ME) principle. Specifically, we first derive the joint probability distribution of the extreme wave heights and the extreme water-levels during a typhoon by using the maximum-entropy principle, and then we nest this distribution with the maximum-entropy distribution of discrete variables to form such a maximum-entropy 2-dimensional (ME 2D) compound distribution model. To further evaluate the performance of our model, we conduct experiments to predict the N-year joint return-periods of the extreme wave heights and the extreme water levels in two areas of the East China Sea. Our experimental results show that our model performs better in predicting in the highly unpredictable joint probability of extreme wave heights and water levels in typhoon affected sea areas, compared with the widely-used Poisson-Mixed-Gumbel model in ocean engineering design.

Acknowledgements

The research work is funded by the National Natural Science Foundation of China Grand No. 51379195, and by the Natural Science Foundation of Shandong Grand No. ZR2013EEM034.

Appendix

Proof:

$$\int_0^{+\infty}\int_0^{+\infty} x^{m_1} f(x,y)\mathrm{d}x\mathrm{d}y = \int_0^{+\infty} x^{m_1}\left(\int_0^{+\infty} f(x,y)\mathrm{d}y\right)\mathrm{d}x = \int_0^{+\infty} x^{m_1} f_x(x)\mathrm{d}x$$

$$\int_0^{+\infty}\int_0^{+\infty} y^{m_2} f(x,y)\mathrm{d}x\mathrm{d}y = \int_0^{+\infty} y^{m_2}\left(\int_0^{+\infty} f(x,y)\mathrm{d}x\right)\mathrm{d}y = \int_0^{+\infty} y^{m_2} f_y(y)\mathrm{d}y$$

where $f_x(x)$ and $f_y(y)$ are the marginal distributions corresponding to $f(x,y)$. Further, according to constraints (6) and (7), we have

$$\int_0^{+\infty}\int_0^{+\infty} (x^{m_1} + y^{m_2}) f(x,y)\mathrm{d}x\mathrm{d}y = c_2 + c_3 < +\infty$$

Because $a^2 + b^2 \geq 2ab$, it follows that

$$x^{m_1} + y^{m_2} = (x^{\frac{m_1}{2}})^2 + (y^{\frac{m_2}{2}})^2 \geq 2x^{\frac{m_1}{2}} y^{\frac{m_2}{2}}$$

then

$$\int_0^{+\infty}\int_0^{+\infty} (x^{\frac{m_1}{2}} y^{\frac{m_2}{2}}) f(x,y)\mathrm{d}x\mathrm{d}y < +\infty$$

It is thus concluded that the constraints (5) and (6) ensure the existence of any order mixed moments of $f(x,y)$ and any order moments of the marginal distributions.

References

[1] K. Emanuel, "Increasing destructiveness of tropical cyclones over the past 30 year", Nature, 2005, 436 (7051): 686-688.

[2] L. Wang, et al., "A new model for calculating the design wave height in typhoon-affected sea areas", Nat Hazar 67 (2): 129-143, 2013.

[3] L. Wang, et al., "A New Method to Estimate Wave Height of Specified Return Period", Chinese Journal of Oceanology and Limnology. 2017, 35 (5).

[4] Y. Cao, et al., "A VEDA simulation on cement paste: using dynamic atomic force microscopy to characterize cellulose nanocrystal distribution", MRS Communications, 7, 2017.

[5] S. Wei, et al., "Analysis of wave motion in one-dimensional structures through fast-Fourier-transform-based wavelet finite element method", Journal of Sound and Vibration 400 (2017): 369-386.

[6] Y. Cao, et al., "The Influence of Cellulose Nanocrystal Additions on the Performance of Cement Paste", Cement and Concrete Composites, 56, p73-83, 2015.

[7] J. Robert, et al., "The influence of cellulose nanocrystals on the microstructure of cement paste", Cement and Concrete Composites, 74, p164-173, 2016.

[8] Y. Cao, et al., "The relationship between cellulose nanocrystal dispersion and strength", Construction and Building Materials, 119, p71–79, 2016.

[9] Z. Zhe, et al., "A thermography-based method for fatigue behavior evaluation of coupling beam damper", Fracture and Structural Integrity 40 (2017): 149-161.

[10] L. Li, et al., "Corrosion Monitoring and Evaluation of Reinforced Concrete Structures Utilizing the Ultrasonic Guided Wave Technique", [J] Distributed Sensor Networks 10, no. 2 (2014).

[11] J. Xu, et al., "Magnetic Transforms of Modulus Type Applied in Regions of Low Latitudes in SE China", Journal of Applied Geophysics. 2017, 139: 188~194.

[12] Z. Zhe, et al., "Optimization Design of Coupling Beam Metal Damper in Shear Wall Structures", Applied Sciences 7, no. 2 (2017): 137.

[13] L. Wang, et al., "Application of linear mean-square estimation in ocean engineering", China Ocean Engineering, 30 (1) 149-160, 2016.

[14] B. Chen, et al., "Overcoming calibration problems in pattern labeling with pairwise ratings: application to personality traits", Computer Vision–ECCV 2016 Workshops, 419-432.

[15] T. Ulrych, "Maximum Entropy Spectral Analysis and Autoregressive Decomposition", Rev Geophysics Space Phys, 1975, 13 (1): 183-200.

[16] J. Xu, et al., "GPR Data Reconstruction Method Based on Compressive Sensing and K-SVD", [J]. Near Surface Geophysics. 2017, 15 (4): 517~524.

[17] V. Ponce-López, et al., "ChaLearn LAP 2016: First Round Challenge on First Impressions-Dataset and Results", Computer Vision–ECCV 2016 Workshops, 400-418.

[18] W. Feller, "An Introduction to Probability Theory and Its Applications (2nd ed)", [M]. New York: John Willey, 1957.

[19] J. Xu, et al., "Sensitivity Analysis of the Influence Factors of Slope Stability Based on LS-SVM", [J]. Geomechanics and Engineering. 2017, 13 (3): 447~458.

[20] L. Li, et al., "Pure density functional for strong correlation and the thermodynamic limit from machine learning", Physical Review B 94.24 (2016): 245129.

[21] J. Xu, et al., "Test and Analysis of Hydraulic Fracture Characteristics of Rock Single Crack", [J]. Fluid Mechanics: Open Access. 2017, 4 (3): 164~167.

[22] J. Xu, et al., "Low Strain Testing of Pile Based on Synchrosqueezing Wavelet Transformation Analysis", [J]. Journal of Vibroengineering. 2016, 18 (2): 813-825.

[23] Q. Ren, et al., "Prediction of the Strength of Concrete Radiation Shielding based on LS-SVM", [J]. Annals of Nuclear Energy. 2015, 85 (0): 296-300.

[24] L. Li, et al. "Understanding machine-learned density functionals", International Journal of Quantum Chemistry 116.11 (2016): 819-833.

[25] J. Xu, et al., "Simulation Analysis of Low Strain Dynamic Testing of Pile with Inhomogeneous Elastic Modulus", [J]. Journal of Measurements in Engineering. 2017, 5 (3): 152~160.